

Isotopic Branching in (He, HD⁺) Collisions[†]

Ashwani Kumar Tiwari, Aditya Narayan Panda, and N. Sathyamurthy*

Department of Chemistry, Indian Institute of Technology Kanpur, Kanpur 208016, India

Received: April 7, 2005

A three-dimensional time-dependent quantum mechanical approach is used to calculate the reaction probability (P^R) and the integral reaction cross section (σ^R) for both channels of the reaction $\text{He} + \text{HD}^+(\nu = 0, 1, 2, 3; j = 0) \rightarrow \text{HeH}(\text{D})^+ + \text{D}(\text{H})$, over a range of translational energy (E_{trans}) on two different ab initio potential energy surfaces (McLaughlin–Thompson–Joseph–Sathyamurthy and Palmieri et al.). The reaction probability plots as a function of translational energy exhibit several oscillations, which are characteristic of the system. The vibrational enhancement of the reaction probability and the integral reaction cross section values are reproduced qualitatively by our calculations, in accordance with the experimental results. The isotopic branching ratio for the reaction decreases in going from $\nu = 0$ to $\nu = 1$ and then becomes nearly ν -independent in going from $\nu = 1$ to $\nu = 3$ on both the surfaces.

I. Introduction

Kinetic isotope effect has been studied by experiment and theory over the years.¹ In elementary chemical reactions, isotopic substitution enables one to probe the interaction potential without changing the system dramatically. The isotopic branching in the reaction $\text{He} + \text{HD}^+ \rightarrow \text{HeH}(\text{D})^+ + \text{D}(\text{H})$ has been studied by several authors. Light and Lin² studied this reaction using phase space theory and showed that, at low total angular momentum (J) values, HeD^+ is the preferred product, whereas, at high J values, HeH^+ would be preferred. Bhalla and Sathyamurthy³ carried out three-dimensional quasiclassical trajectory (QCT) calculations using the McLaughlin–Thompson–Joseph–Sathyamurthy (MTJS) potential-energy surface (PES)^{4,5} and reported the preferential formation of HeD^+ over HeH^+ for vibrational (ν) states 0–4, (rotational state $j = 0$) over a wide range of translational energy (E_{trans}). Kumar et al.⁶ also carried out three-dimensional QCT calculations and found that the isotopic branching ratio $\Gamma = \sigma^R(\text{HeH}^+)/\sigma^R(\text{HeD}^+)$, where σ^R refers to the integral reaction cross section, was less than unity for $\nu = 0$ –3 but slightly greater than one for certain values of E_{trans} for $\nu = 4$.

Mahapatra and Sathyamurthy⁷ investigated the dynamics of collinear (He, HD⁺) collisions using the time-dependent quantum mechanical (TDQM) approach^{8,9} on the MTJS surface and found that there were a large number of reactive scattering resonances for HeH^+ and HeD^+ formation. However, the reaction probability (P^R) for HeH^+ showed a staircaselike structure, when plotted as a function of total energy (E) for different vibrational states. For the HeD^+ channel, however, $P^R(E)$ varied in a highly oscillatory manner. Further investigation revealed larger lifetimes for quassibound states of $[\text{HeDH}]^+$ than for $[\text{HeHD}]^+$.¹⁰

Preliminary studies by Balakrishnan and Sathyamurthy¹¹ for (He, HD⁺) collisions on the MTJS surface using the TDQM methodology in hyperspherical coordinates for total angular momentum ($J = 0$) revealed that HeD^+ was formed preferentially over HeH^+ , and hence the isotopic branching ratio $\Gamma =$

$P^R(\text{HeH}^+)/P^R(\text{HeD}^+)$ was less than unity for different vibrational states over a range of E_{trans} . A more detailed investigation by Kalyanaraman et al.¹² showed that there were a large number of reactive scattering resonances in three-dimensional (He, HD⁺) collisions for $J = 0$ and that Γ oscillated as a function of E_{trans} for $0.95 \leq E_{\text{trans}} \leq 1.5$ eV and was less than unity for $E_{\text{trans}} > 1.0$ eV, for $\nu = 0, j = 0$. For all other $\nu (=1-3)$ states, Γ was less than unity over the entire energy range. It was not clear if these oscillations would survive on J -averaging and if J -weighted Γ would depend on the initial rotational state j .

Unfortunately, experimental studies on (He, HD⁺) collisions have been rather limited. Klein and Friedman¹³ investigated the system experimentally and reported that the branching ratio Γ decreased with increase in E_{trans} . Turner et al.¹⁴ also investigated the system experimentally over a range of E_{trans} and found that Γ was less than unity for $\nu = 0$ –2, but exceeded one for $\nu = 3$ and 4 at $E_{\text{trans}} = 1.0$ eV.

To test theory against experiment we had undertaken a detailed three-dimensional TDQM study of the E_{trans} -dependence of $\sigma^R(\text{HeH}^+)$ and $\sigma^R(\text{HeD}^+)$ and also of Γ for $\nu = 0, 1, 2$, and 3 for $j = 0$ on the MTJS PES. In the meantime a slightly more accurate PES for the system was published by Palmieri et al.¹⁵ Therefore we repeated the TDQM calculations on the Palmieri et al. PES to determine if our findings were PES-dependent. Details of the methodology are given in section II, and the results obtained are presented and discussed in section III. This is followed by a summary and conclusion in section IV.

II. Methodology

The TDQM methodology involves solving the time-dependent Schrödinger equation in reactant channel Jacobi coordinates on an L-shape grid.^{16,17} For $j = 0$ of HD⁺, the Hamiltonian operator in (R, r, γ) space is given as¹⁸

$$H = -\frac{\hbar^2}{2\mu_R} \frac{\partial^2}{\partial R^2} - \frac{\hbar^2}{2\mu_r} \frac{\partial^2}{\partial r^2} + \frac{\mathbf{J}^2}{2\mu_r R^2} + V(R, r, \gamma) \quad (1)$$

where μ_R is the reduced mass of He with respect to the center-of-mass of HD⁺ and μ_r is the reduced mass of HD⁺. R is the center of mass separation between He and HD⁺, r is the

[†] Part of the special issue "Donald G. Truhlar Festschrift".

* E-mail for correspondence: nsath@iitk.ac.in.

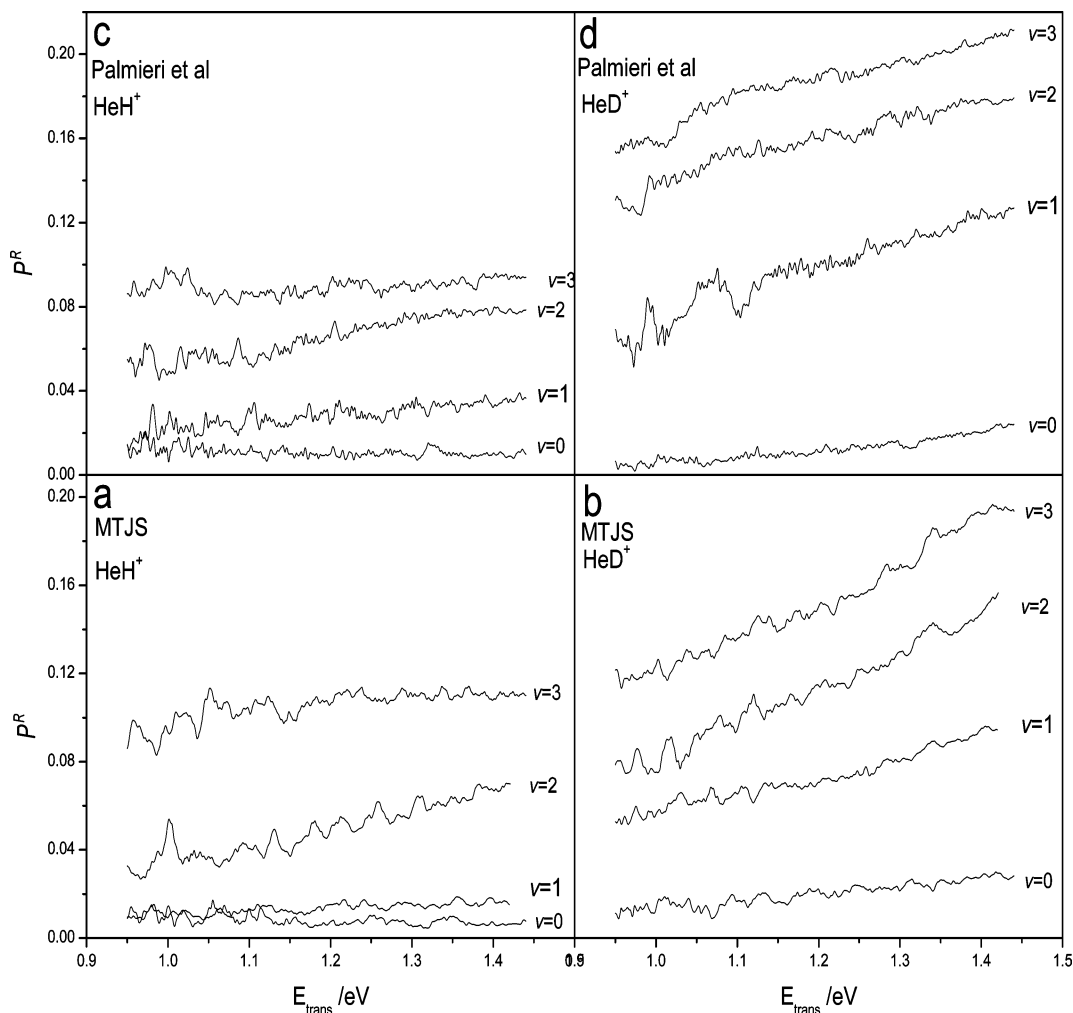


Figure 1. Reaction probability values plotted as a function of E_{trans} on both surfaces for $J = 0$; $v = 0, 1, 2,$ and 3 ; $j = 0$ for both product channels, HeH^+ and HeD^+ .

separation between H and D, and γ is the angle between R and r . \mathbf{J} is the total angular momentum operator, and $V(R, r, \gamma)$ is the interaction potential.

The initial wave packet for the time evolution was chosen as

$$\psi(R, r, \gamma, t=0) = G_{k_0}(R) \phi_{vj}(r) P_{jK}(\cos \gamma) \quad (2)$$

$$G_{k_0} = \left(\frac{1}{\pi \delta^2} \right)^{1/4} \exp\{-(R-R_0)^2/2\delta^2\} \exp(-ik_0 R) \quad (3)$$

where R_0 and k_0 refer to the center of the wave packet in position and momentum coordinate, respectively. δ is the width parameter for the wave packet, K is the projection of J on the body fixed z axis, and $P_{jK}(\cos \gamma)$ represents the associated Legendre polynomials.

The diatomic rovibrational eigenfunctions $\phi_{vj}(r)$ for HD^+ are computed by means of the Fourier grid Hamiltonian approach proposed by Marston and Balint-Kurti.¹⁹

The split-operator method²⁰ was used to propagate the wave packet in time. The fast Fourier transform (FFT) method²¹ was used to solve the radial part of the Schrödinger equation, and the discrete variable representation (DVR)²² was used for the angular part. The time-dependent Schrödinger equation was solved under centrifugal sudden approximation,²³ and the wave packet was propagated for 0.97–1.93 ps. Having computed $\psi(R,$

$r, \gamma, t)$ at time t , the energy resolved reaction probability $P_{vj}^R(E)$ was calculated as¹²

$$P_{vj}^R(E) = \frac{\hbar}{\mu_r} \text{Im} \left[\int_0^\infty dR \int_0^\pi d\gamma \sin \gamma \psi^*(R, r, \gamma, E) \frac{d}{dr} \psi(R, r, \gamma, E) \right]_{r=r_s} \quad (4)$$

where the energy-dependent wave function $\psi(R, r, \gamma, E)$ was obtained by Fourier transforming the time-dependent wave packet $\psi(R, r, \gamma, t)$.

For computing reaction probabilities corresponding to the HeH^+ and HeD^+ channels, r_s has been taken to be sufficiently large and away from the interaction region. Depending upon the magnitude of r_{HeH^+} and r_{HeD^+} , the flux was integrated into either of the two channels. It was verified that the sum of the reaction probabilities obtained from individual product channels and the total reaction probability obtained directly from the energy-resolved flux out of the reactant channel were the same.

The J -dependent initial state-selected partial reaction cross section σ_{vj}^J was determined as

$$\sigma_{vj}^J(E) = \frac{1}{(2j+1)} [P_{vj}^{JK=0}(E) + 2 \sum_{K=1}^j P_{vj}^{JK}(E)] \quad (5)$$

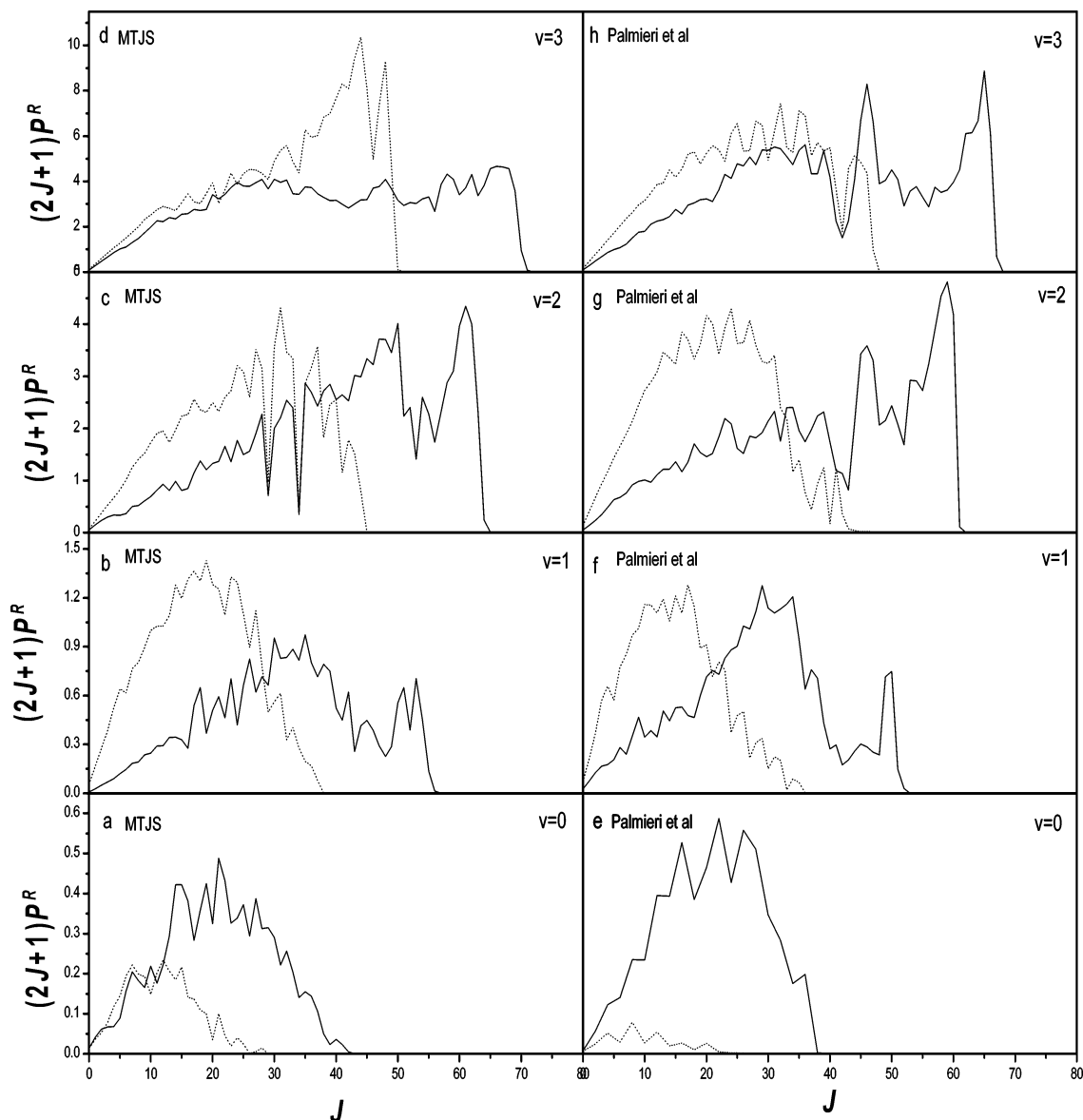


Figure 2. $(2J + 1) P^R$ values plotted as a function of J for HeH^+ (—) and HeD^+ (....) channels obtained from the MTJS (a, b, c, and d) and Palmieri et al. (e, f, g, and h) PESs for $v = 0, 1, 2,$ and $3; j = 0$ of HD^+ at $E_{\text{trans}} = 1.0$ eV.

The initial state-selected total reaction cross section $\sigma_{vj}(E)$ was then obtained by summing over the partial reaction cross section values for all the partial waves:

$$\sigma_{vj}(E) = \frac{\pi}{k_{vj}^2} \sum_{J=0}^{J_{\text{max}}} (2J + 1) \sigma_{vj}^J(E) \quad (6)$$

Further details of the methodology can be seen in our earlier publication.²⁴

III. Results and Discussion

A. Reaction Probabilities. Computed P^R values as a function of E_{trans} on both surfaces are plotted for $J = 0; v = 0, 1, 2, 3; j = 0$ for both product channels, HeH^+ and HeD^+ in Figure 1. There are a large number of oscillations in $P^R(E)$ for both channels indicating the importance of resonances in the dynamics of the (He, HD^+) collisions. It is clear that, over the entire translational energy range, HeD^+ is preferred over HeH^+ for $J = 0$, in agreement with the earlier results of Balakrishnan and Sathyamurthy.¹¹ This is presumably due to the fact that, after

the formation of the complex HeHD^+ , the lighter H atom is able to recede more rapidly than the heavier D atom. Also, a larger cone-of-acceptance at the D end due to a shift in the center-of-mass of HD^+ favors the formation of HeD^+ . Further, there is an overall increase in P^R with an increase in E_{trans} for HeD^+ , whereas, for HeH^+ , it does not change too much with an increase in E_{trans} . For both channels, the vibrational enhancement of the reaction probability values can be seen clearly in Figure 1.

The partial reaction cross section $[(2J + 1)P^R]$ values for HeH^+ and HeD^+ channels obtained from the MTJS and Palmieri et al. PESs are plotted as a function of J for $v = 0, 1, 2, 3; j = 0$ at $E_{\text{trans}} = 1.0$ eV in Figure 2. It is clear that HeD^+ is formed preferentially over HeH^+ at low J values and that at high J values the trend is reversed on both surfaces for all v except for $v = 0$ on the Palmieri et al. PES, where HeH^+ is preferred over HeD^+ over all the J values. For $j = 0$, the total angular momentum and hence the orbital angular momentum are directly proportional to the impact parameter (b) and the latter is related to the scattering angle for direct collisions. As $b \rightarrow 0$, the scattering will be in the backward direction, and for large b ,

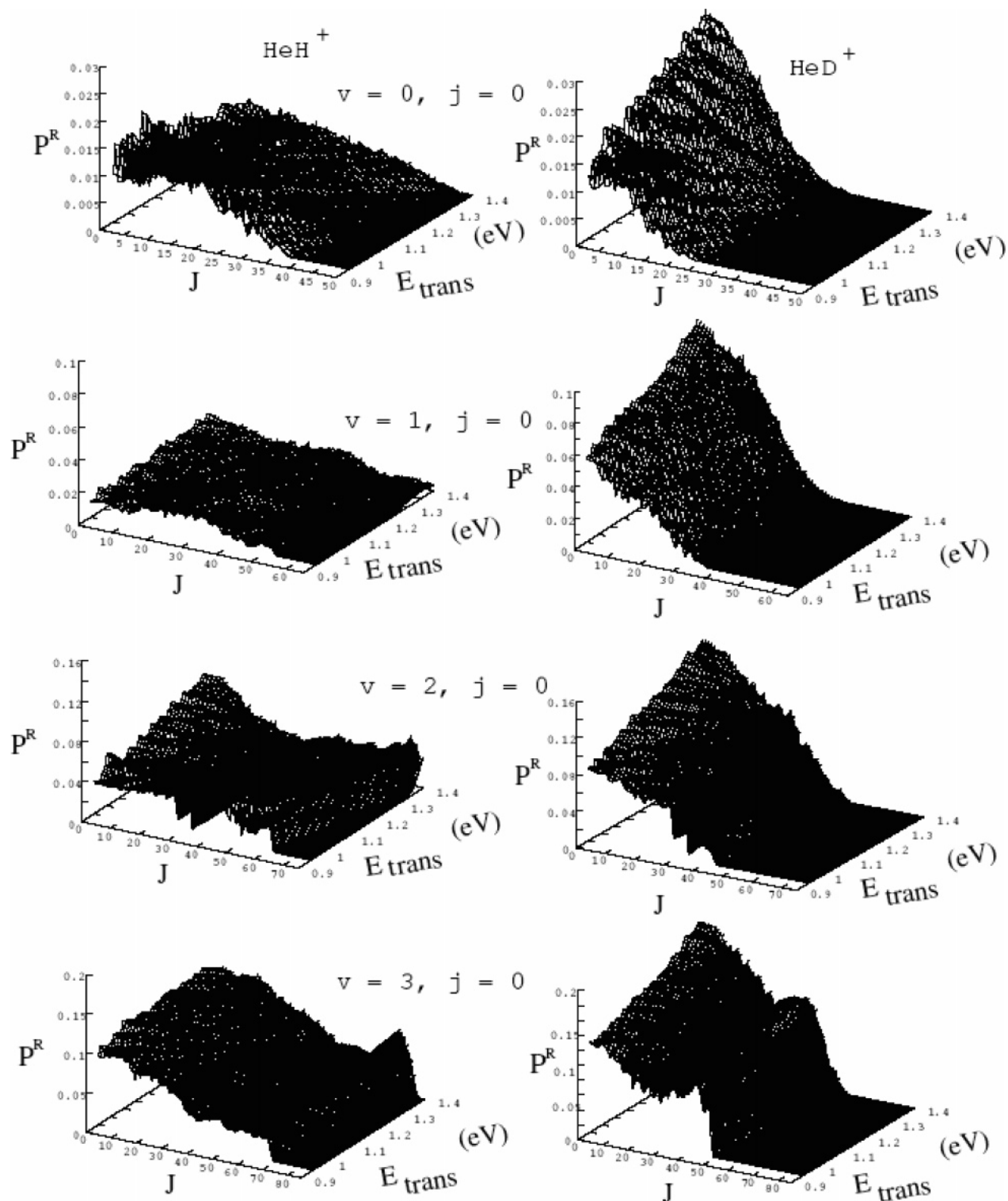


Figure 3. P^R values plotted as a function of J and E_{trans} for HeH⁺ channel (left panel) and HeD⁺ channel (right panel) for $v = 0, 1, 2$, and $3; j = 0$ of HD⁺ on MTJS PES.

the scattering will be in the forward direction. Therefore, we infer that HeH⁺ would be scattered preferentially in the forward direction and HeD⁺ would be scattered in the backward direction for $v = 1, 2, 3$. For $v = 0$, the MTJS PES gives a slight preference to HeD⁺ over HeH⁺ up to $J = 9$ but a larger preference to HeH⁺ over HeD⁺ for $J > 9$. On the Palmieri et al. PES, on the other hand, HeH⁺ is preferred over HeD⁺ for all J values. The partial reaction cross section plots have similar structures on both surfaces. Also the maximum value of J (J_{max})

for which P^R becomes zero is nearly the same for all the vibrational levels, for both the channels on both surfaces.

To examine the sensitivity of P^R to J and E_{trans} , the P^R values are plotted for HeH⁺ and HeD⁺ channels as a function of J and E_{trans} in Figures 3 and 4, respectively, for the MTJS and the Palmieri et al. PESs. It is clear that for a given (v, j) the plots for each channel have very similar structures on both surfaces. P^R for HeH⁺ decreases slowly with an increase in J , whereas it decreases rapidly for the HeD⁺ channel. Further there

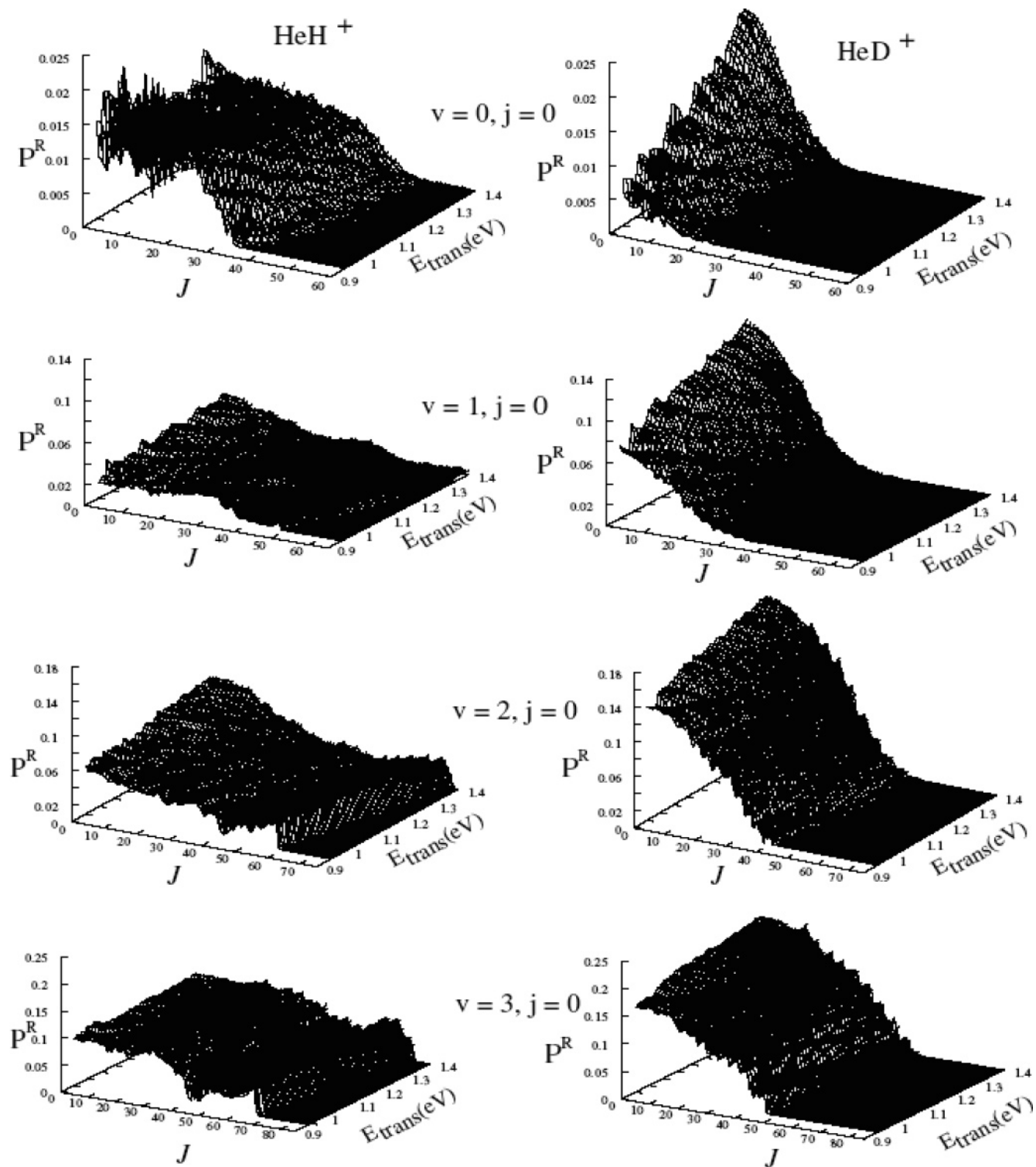


Figure 4. Same as in Figure 3 for the Palmieri et al. PES.

is not much overall increase in P^R with an increase in E_{trans} for the HeH⁺ channel. For HeD⁺ channel, on the other hand, there is a larger overall increase in P^R with an increase in E_{trans} . Also at a given E_{trans} , J_{max} for HeH⁺ channel is larger than J_{max} for HeD⁺ for all v states. It is also clear that with increase in J , the reaction threshold increases for both the channels. Vibrational enhancement in P^R and an increase in J_{max} with an increase in v can also be seen in Figures 3 and 4.

B. Reaction Cross Section and Isotopic Branching Ratios.

After computing the reaction probabilities for a large number of J values, the integral reaction cross section for the formation

of HeH⁺ and HeD⁺ has been calculated, for $v = 0, 1, 2, 3$. The resulting integral reaction cross section values are plotted in Figure 5 for HeH⁺ and HeD⁺ formation on both the MTJS PES and Palmieri et al. PES, along with the experimental values at $E_{trans} = 1.0$ eV. The total integral reaction cross section is also plotted in the same figure. Vibrational enhancement of the integral reaction cross section is evident for both product channels. The excitation function plots are very similar on both surfaces, and they do not show any substantial increase in σ^R with an increase in E_{trans} on both surfaces, particularly for $v = 0, 1, 2$. The TDQM results are compared with the available

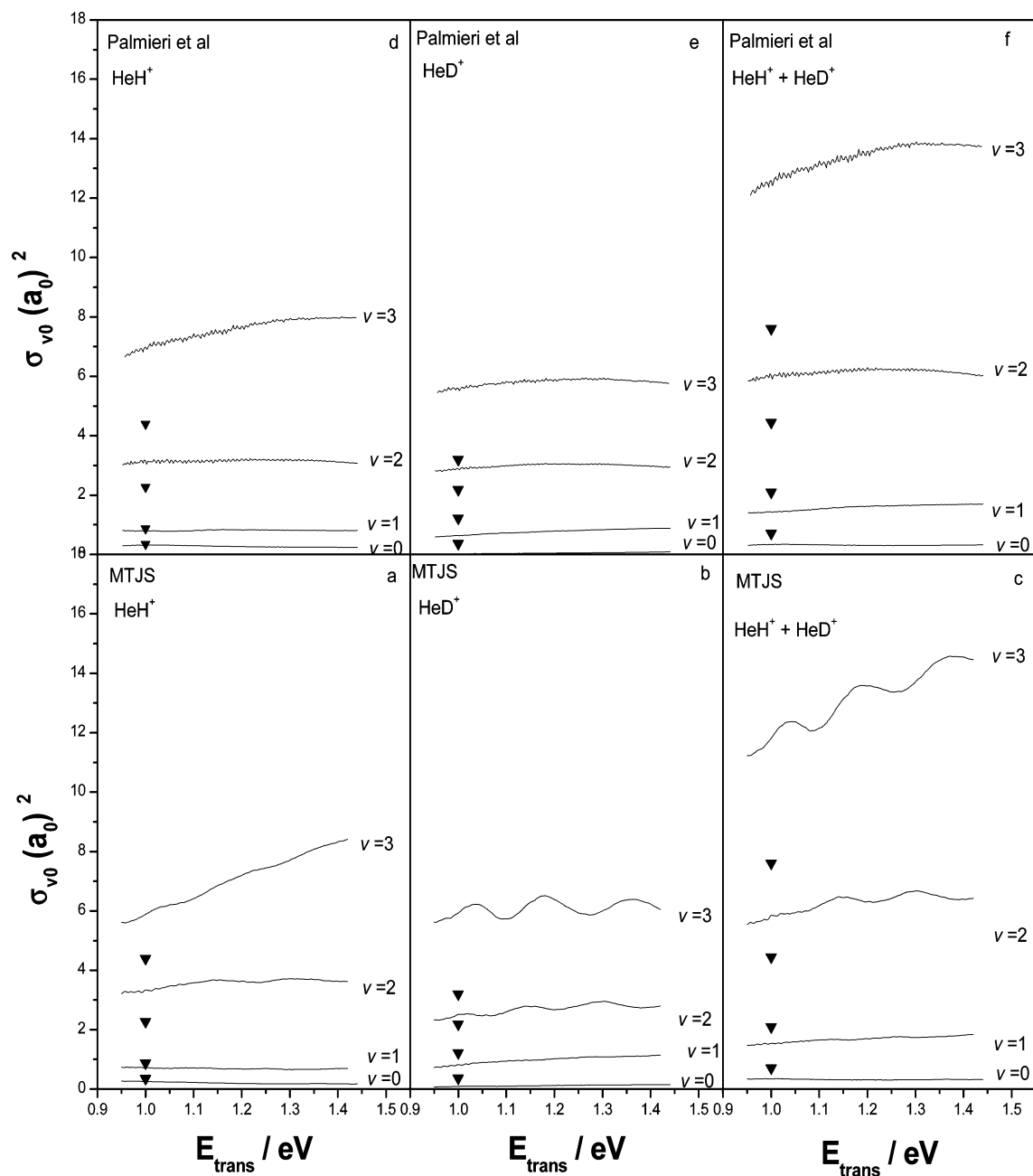


Figure 5. Integral reaction cross section plotted as a function of E_{trans} for HeH^+ and HeD^+ channels on both the surfaces for $\nu = 0, 1, 2$ and 3 ; $j = 0$ of HD^+ along with experimental results (\blacktriangledown) at $E_{trans} = 1.0$ eV.

experimental results at $E_{trans} = 1.0$ eV.¹⁴ It is clear that the TDQM calculation overestimates the reaction cross section for $\nu = 2$ and $\nu = 3$, when compared to the experimental results for both channels. Here, one must bear in mind that the experimental results are j -weighted, whereas the theoretical calculation is only for $j = 0$.

The isotopic branching ratio [$\Gamma = \sigma^R(\text{HeH}^+)/\sigma^R(\text{HeD}^+)$] is plotted as a function of E_{trans} in Figure 6 for both surfaces. It is clear that, for $\nu = 0$, Γ is very large at small energy, and it decreases dramatically with increase in energy. Also for $\nu = 0$, the branching ratio obtained from the Palmieri et al. PES is higher than that calculated from the MTJS. This is presumably due to fact that Γ is a ratio of two small values for $\nu = 0$. Γ for $\nu = 1, 2, 3$ is nearly independent of energy. The computed Γ values are compared with the experimental results at $E_{trans} = 1.0$ eV, in Figure 7. It is clear that there is very good agreement between experiment and theory on both surfaces for all ν values except $\nu = 0$.

Recently, Baer²⁵ and Zhang et al.²⁶ have reported the isotopic branching ratio in $\text{F} + \text{HD}$ collisions. Both the TIQM results of Baer and TDQM results of Zhang et al. showed the product HF to be formed preferentially over DF in a low collision energy range. This they attributed to the lower mass of H, which tunnels easily through the thin barrier of the PES compared to the heavier D atom. With an increase in collision energy, TDQM results showed DF to be the preferred product. Our findings are consistent with their results.

IV. Summary and Conclusions

Initial state-selected integral reaction cross section values for $\text{He} + \text{HD}^+ (\nu = 0, 1, 2, 3; j = 0) \rightarrow \text{HeH(D)}^+ + \text{D(H)}$ have been computed using a time-dependent quantum mechanical wave packet approach on two different ab initio potential energy surfaces, within the centrifugal sudden approximation. Vibrational enhancement of the reaction cross section observed in

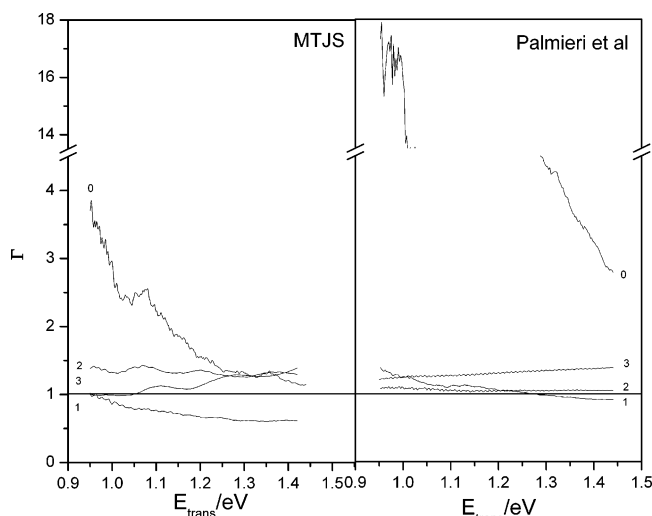


Figure 6. Isotopic branching ratio plotted as a function of E_{trans} on both surfaces for $v = 0, 1, 2,$ and $3; j = 0$.

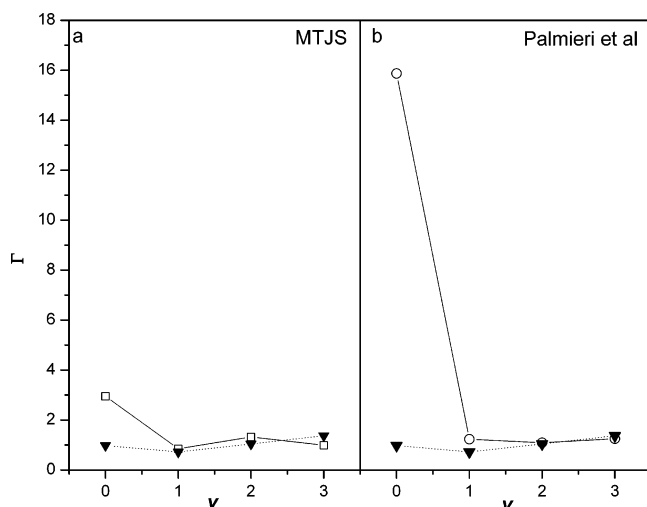


Figure 7. Isotopic branching ratio plotted as a function of v on both surfaces along with experimental results (▼) at $E_{trans} = 1.0$ eV.

experiments is reproduced qualitatively by our calculations for both product channels. Plots of P^R as a function of E_{trans} exhibit characteristic oscillations. The isotopic branching ratio decreases in going from $v = 0$ to $v = 1$, and then it becomes nearly independent of v in going from $v = 1$ to $v = 3$ for $j = 0$. It

would be worth doing additional calculations for higher j values to examine the influence of j on Γ . Also the effect of adding the Coriolis coupling on the integral reaction cross section needs to be examined. These studies are under progress, and the results will be published subsequently.

Acknowledgment. One of us (A.K.T.) would like to thank the Council of Scientific and Industrial Research (CSIR), New Delhi for a research fellowship. This study was supported in part by a grant from CSIR, New Delhi.

References and Notes

- (1) March, J. *Advanced Organic Chemistry*, 4th ed.; Wiley: New York, 1992; p 226.
- (2) Light, J. C.; Lin, J. *J. Chem. Phys.* **1965**, *43*, 3209.
- (3) Bhalla, K. C.; Sathyamurthy, N. *Chem. Phys. Lett.* **1989**, *160*, 437.
- (4) McLaughlin, D. R.; Thompson, D. L. *J. Chem. Phys.* **1979**, *70*, 2748.
- (5) Joseph, T.; Sathyamurthy, N. *J. Chem. Phys.* **1987**, *86*, 704.
- (6) Kumar, S.; Sathyamurthy, N.; Bhalla, K. C. *J. Chem. Phys.* **1993**, *98*, 4660.
- (7) Mahapatra, S.; Sathyamurthy, N. *J. Chem. Phys.* **1996**, *105*, 10934.
- (8) Balakrishnan, N.; Kalyanaraman, C.; Sathyamurthy, N. *Phys. Rep.* **1997**, *280*, 79.
- (9) Zhang, J. Z. H. *Theory and Application of Quantum Molecular Dynamics*; World Scientific: Singapore, 1999.
- (10) Mahapatra, S.; Sathyamurthy, N.; Ramaswamy, R. *Pramana* **1997**, *48*, 411.
- (11) Balakrishnan, N.; Sathyamurthy, N. *Proc. Indian Acad. Sci., Chem. Sci.* **1994**, *106*, 531.
- (12) Kalyanaraman, C.; Clary, D. C.; Sathyamurthy, N. *J. Chem. Phys.* **1999**, *111*, 10910.
- (13) Klein, F. S.; Friedman, L. *J. Chem. Phys.* **1964**, *41*, 1789.
- (14) Turner, T.; Dutuit, O.; Lee, Y. T. *J. Chem. Phys.* **1984**, *81*, 3475.
- (15) Palmieri, P.; Puzzarini, C.; Aquilanti, V.; Capecchi, G.; Cavalli, S.; De Fazio, D.; Aguilar, A.; Gimenez, X.; Lucas, J. M. *Mol. Phys.* **2000**, *98*, 1835.
- (16) Mowrey, R. C.; Kouri, D. J. *J. Chem. Phys.* **1986**, *84*, 6466.
- (17) Mowrey, R. C. *J. Chem. Phys.* **1991**, *94*, 7078; **1993**, *99*, 7049.
- (18) Gögtas, F.; Balint-Kurti, G. G.; Offer, A. R. *J. Chem. Phys.* **1996**, *104*, 7927.
- (19) Marston, C. C.; Balint-Kurti, G. G. *J. Chem. Phys.* **1989**, *91*, 3571.
- (20) Feit, M. D.; Fleck, J. A., Jr.; Steiger, A. *J. Chem. Phys.* **1982**, *47*, 412.
- (21) Kosloff, D.; Kosloff, R. *J. Comput. Phys.* **1983**, *52*, 35.
- (22) Parker, G. A.; Light, J. C. *Chem. Phys. Lett.* **1982**, *89*, 483. Light, J. C.; Hamilton, I. P.; Lill, J. V. *J. Chem. Phys.* **1985**, *82*, 1400.
- (23) Pack, R. T. *J. Chem. Phys.* **1974**, *60*, 633.
- (24) Maiti, B.; Kalyanaraman, C.; Panda, A. N.; Sathyamurthy, N. *J. Chem. Phys.* **2002**, *117*, 9719.
- (25) Baer, M. *Chem. Phys. Lett.* **1999**, *312*, 203.
- (26) Zhang, D. H.; Lee, S.; Baer, M. *J. Chem. Phys.* **2000**, *112*, 9802.